Spectroscopic factor strengths using *ab initio* approaches

P. C. Srivastava* and Vikas Kumar
Department of Physics, Indian Institute of Technology, Roorkee 247 667, India
(Received 24 July 2016; revised manuscript received 8 October 2016; published 5 December 2016)

We have calculated the spectroscopic factor strengths for the one-proton and one-neutron pick-up reactions ^{27}Al$(d,^3$He$)^{26}$Mg and ^{27}Al$(d,t)^{26}$Al within the framework of the shell model. We employed two different *ab initio* approaches: an in-medium similarity renormalization targeted for a particular nucleus, and the coupled-cluster effective interaction. We also compared our results with recently determined experimental spectroscopic factors.

DOI: 10.1103/PhysRevC.94.064306

I. INTRODUCTION

The nature and occupancy of the single-particle orbits for a nucleus can be determined from the spectroscopic factors (SFs). Experimentally the SFs can be measured with single-particle transfer reactions. These reactions are of two types, the first one is stripping in which one nucleon is stripped from the incoming projectile, while the second one is a pick-up reaction in which one nucleon is picked up by the projectile. The examples of neutron transfer pick-up reactions are (p,d), (d,t), and $(^3$He $,\alpha)$, while stripping reactions are (d,p), (t,d), and $(\alpha,^3$He$)$ [1]. The SF is defined by a matrix element between the initial and final states corresponding to entrance and exit channels, respectively. It is possible to describe the capture or emission of single nucleons in stellar burning processes by calculating the nuclear matrix elements for single-nucleon spectroscopic factors in the nuclear structure calculations.

Studies of SFs in different regions of the nuclear chart are reported in Refs. [2–8]. Surveys of excited state neutron spectroscopic factors for $Z = 8-28$ nuclei are reported by Tsang *et al.* [9]. In that work they extracted 565 neutron SFs for sd and fp shell nuclei by analyzing (d,p) angular distributions, they also compared the experimental results with shell-model results.

To study different excited states and their spectroscopic factors for ^{26}Mg, many experimental results were reported earlier in Refs. [10–16]. Recently, the spectroscopic factors for ^{26}Mg were reported in Ref. [17] using the ^{27}Al$(d,^3$He$)^{26}$Mg reaction. The structure of ^{27}Al deduced from experiments which enlighten different reaction channels were reported in Refs. [18–24]. The experimental results for SFs of 14 excited states for ^{27}Al using the ^{27}Al$(d,t)^{26}$Al reaction are reported in Ref. [25]. The studies of ^{26}Al and ^{26}Mg are important for the astrophysics point of view. The massive stars throughout the Galaxy dominate in the production of ^{26}Al [26], and it decays by β^+ to ^{26}Mg.

In the present work we have performed shell-model calculations using *ab initio* approaches for one-neutron and one-proton pick-up reactions on ^{27}Al within the framework of the shell model.

II. *AB INITIO* SHELL-MODEL ANALYSIS

We performed shell-model calculations using two modern approaches: an in-medium similarity renormalization targeted for a particular nucleus [27] and the *ab initio* coupled-cluster effective interaction (CCEI) [28]. We also compared results with phenomenological USDB interaction [29]. For the diagonalization of matrices we used the shell-model code NUSHELLX [30].

Recently, Stroberg *et al.* reported mass-dependent Hamiltonians for sd-shell nuclei using the in-medium similarity renormalization group (IM-SRG) based on chiral two- and three-nucleon interactions [31]. Further extension has been done for *ab initio* IM-SRG calculations based on ensemble reference states to consider residual NNN forces among valence nucleons. This is a nucleus-dependent valence-space approach to study nuclear structure properties [27]. In the present work we performed calculations for the spectroscopic factor strengths using separate effective interactions for ^{26}Mg, ^{26}Al, and ^{27}Al based on nucleus-dependent valence space [27].

The *ab initio* coupled-cluster effective interaction (CCEI) [28] uses the A-dependent Hamiltonian

$$\hat{H} = \sum_{i<j}\left(\frac{(\mathbf{p}_i - \mathbf{p}_j)^2}{2mA} + \hat{V}_{NN}^{(i,j)}\right) + \sum_{i<j<k}\hat{V}_{3\mathrm{N}}^{(i,j,k)}, \quad (1)$$

with an initial next-to-next-to-next-to-leading order (N3LO) chiral NN interaction, and next-to-next-to-leading order (N2LO) local chiral NNN interaction, using similarity renormalization group transformation. From this the shell-model Hamiltonian in a sd valence space obtained from *ab initio* coupled-cluster theory. Where the CCEI Hamiltonian is

$$H_{\mathrm{CCEI}} = H_0^{A_c} + H_1^{A_c+1} + H_2^{A_c+2} + \cdots . \quad (2)$$

For the shell-model space this Hamiltonian is limited for one- and two-body terms. The two-body term is computed using the Okubo-Lee-Suzuki similarity transformation. In Eq. (2), A is the mass of the nucleus, A_c is the mass of core, $H_0^{A_c}$ is the Hamiltonian for the core, $H_1^{A_c+1}$ is the valence one-body Hamiltonian, and $H_2^{A_c+2}$ is the additional two-body Hamiltonian. Coupled-cluster theory results for spectroscopic factors for proton and neutron removal from ^{16}O are reported in Ref. [32].

*pcsrifph@iitr.ac.in

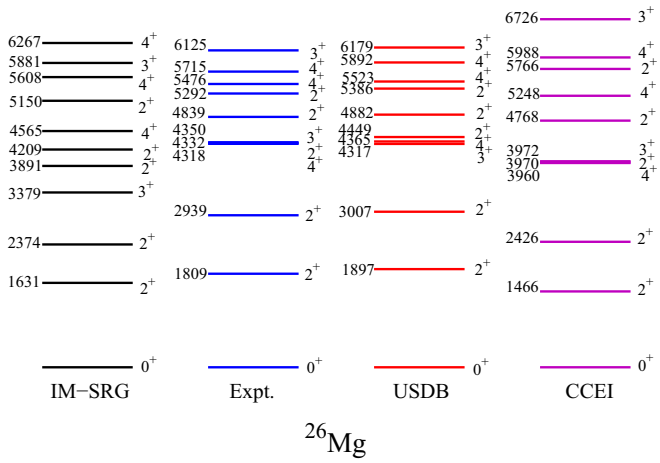

FIG. 1. Comparison between calculated energy levels and experimental data for ^{26}Mg.

The Hamiltonian of the USDB interaction is based on a renormalized G matrix by fitting two-body matrix elements with experimental data for binding energies and excitation energies for the sd-shell nuclei [29,33]. The USDB interaction is fitted by varying 56 linear combinations of two-body matrix elements. The rms deviations of 130 keV were obtained between experimental and theoretical energies for the USDB interaction. In the present work before calculating the SFs, first we examined the wave functions of concerned nuclei using IM-SRG, CCEI, and USDB effective interactions. The comparison between the calculated and experimental levels for ^{26}Mg and ^{26}Al is reported in Figs. 1 and 2. The results of the USDB interaction are much better than those for the IM-SRG and CCEI interactions. In the case of ^{26}Al we calculated only the g.s.(0^+).

We can define the spectroscopic amplitudes for pick-up and stripping reactions by taking the expectation values of the operators $a\dagger$ and a between the states of nuclei with $A-1$ and A, and $A+1$ and A. The spectroscopic factor in terms of the

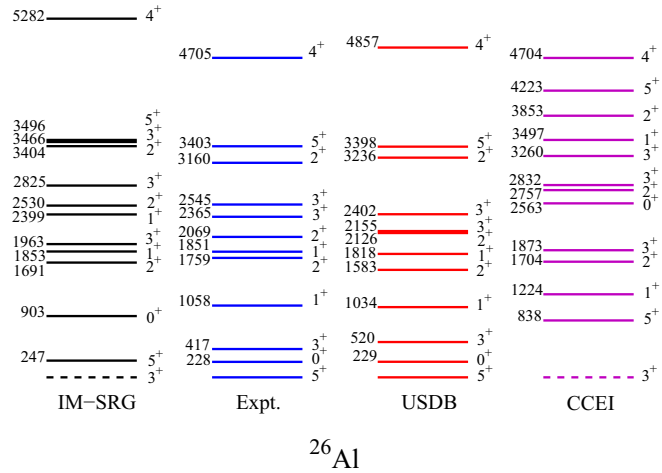

FIG. 2. Comparison between calculated energy levels and experimental data for ^{26}Al.

reduced matrix elements of $a\dagger$ is given by

$$S = \frac{1}{2J+1}\,|\langle \psi^A \omega J||a_k^\dagger||\psi^{A-1}\omega' J'\rangle|^2, \tag{3}$$

where the $(2J+1)$ factor is by convention associated with a heavier mass A. Here the ω indices distinguish the various basis states with the same J value [34,35].

Experimentally [17,25], the spectroscopic factors of different states were extracted using the relation between experimental cross section and theoretical cross sections

$$\left(\frac{d\sigma}{d\Omega}\right)_{\text{expt}} = 3.33\frac{C^2S}{2J+1}\left(\frac{d\sigma}{d\Omega}\right)_{\text{DWBA}}, \tag{4}$$

where $(\frac{d\sigma}{d\Omega})_{\text{expt}}$ is the experimental differential cross section and $(\frac{d\sigma}{d\Omega})_{\text{DWBA}}$ is the cross section predicted by the DWUCK4 code. J $(J = l \pm \frac{1}{2})$ is the total angular momentum of the orbital from where the proton is picked up. C^2 is the isospin Clebsch-Gordon coefficient and S is the spectroscopic factor.

The uncertainty in the experimental SFs may be due to following: (i) the zero-range parameter D_0 may be uncertain, (ii) the optical potential may be uncertain, (iii) the zero-range distorted-wave Born-approximation (DWBA) is not sufficient [36–38]. In Refs. [17,25], it was reported that the replacement of the zero-range approximation with finite-range and nonlocal parameters reduces the SFs up to 45–50%.

Furnstahl and Hameer, using effective field theory, tried to determine whether occupation numbers and momentum distributions of nucleons in nuclei are observables. They claimed that these quantities can only be defined if we take specific forms of the Hamiltonian, regularization scheme, etc. [39]. In effective field theory, there is no definite form of the Hamiltonian, thus it is not possible to define occupation numbers (or even momentum distribution). The "nonobservable" nuclear quantities such as momentum distribution and spectroscopic factor using parton distribution function (PDFs) are reported in Ref. [40]. The inclusion of long-range (low-momentum) pion-exchange tensor forces is important. But the recent study for the quenching of spectroscopic factors suggests that a long-range correlation is more dominating [41]. The uncertainty of the SFs coming from different sources was reported in the review article by Dickhoff and Barbieri [42]. Inelastic proton scattering is a surface reaction, thus no detailed information is obtained related to the interior of the nucleus; this will gives rise to an error of 10%. Another uncertainty is due to the choice of the electron-proton cross section; this will give a small uncertainty in the analysis of low-Q^2 data.

A. Calculation of C^2S for $1p$ pick-up reaction ^{27}Al$(d,{}^3$He$)^{26}$Mg

Experimentally the states of ^{26}Mg [17] were studied by assuming pick-up from the $d_{5/2}$ orbital only, and also a few states by assuming configuration mixing of the two lower orbitals of the sd shell: $d_{5/2}$ and $s_{1/2}$ single-particle orbitals. In Table I, we compared the experimental C^2S values with shell-model results for IM-SRG, CCEI, and USDB interactions (the corresponding wave functions are shown in Table II). As extracted from experiment the calculated C^2S values were very large for $l=2$ $(d_{5/2})$ transfer as compared with $l=0$

TABLE I. Extracted values of C^2S for different excited states of ^{26}Mg from the reaction ^{27}Al(d,^{3}He) at 25 MeV. Experimental data are from Ref. [17]. Here $l = 0$ and $l = 2$ are for $s_{1/2}$ and $d_{5/2}$ orbitals, respectively.

Expt.	J^π	[USDB]	[IM-SRG]	[CCEI]	C^2S[Expt.]		C^2S[USDB]		C^2S[IM-SRG]		C^2S[CCEI]	
keV		keV	keV	keV	$l=0$	$l=2$	$l=0$	$l=2$	$l=0$	$l=2$	$l=0$	$l=2$
0	0^+_1	$0(0^+_1)$	$0(0^+_1)$	$0(0^+_1)$		0.17 ± 0.05		0.276		0.232		0.339
1806	2^+_1	$1897(2^+_1)$	$1631(2^+_1)$	$1466(2^+_1)$	0.002	0.57 ± 0.14	0.014	0.876	0.006	0.647	0.036	0.140
2935	2^+_2	$3007(2^+_2)$	$2374(2^+_2)$	$2426(2^+_2)$	0.002	0.13 ± 0.03	0.021	0.090	0.030	0.072	0.002	0.170
	3^+_1	$4317(3^+_2)$	$3379(3^+_1)$	$3972(3^+_1)$			0.072	0.005	0.0002	0.0001	0.055	0.000
	4^+_1	$4365(4^+_1)$	$4565(4^+_1)$	$3960(4^+_1)$				1.620		1.038		0.795
	2^+_3	$4449(2^+_3)$	$3891(2^+_3)$	$3970(2^+_3)$			0.044	0.074	0.0002	0.057	0.016	0.196
	2^+_4	$4882(2^+_4)$	$4209(2^+_4)$	$4768(2^+_4)$			0.140	0.022	0.220	0.053	0.078	0.091
	2^+_5	$5386(2^+_5)$	$5150(2^+_5)$	$5766(2^+_5)$			0.009	0.004	0.103	0.024	0.205	0.122
	4^+_2	$5523(4^+_3)$	$5608(4^+_4)$	$5248(4^+_3)$				0.185		0.030		0.009
	4^+_3	$5892(4^+_4)$	$6267(4^+_5)$	$5988(4^+_4)$				0.001		0.030		0.025
	3^+_2	$6179(3^+_3)$	$5881(3^+_3)$	$6726(3^+_3)$			0.028	0.006	0.067	0.022	0.185	0.002

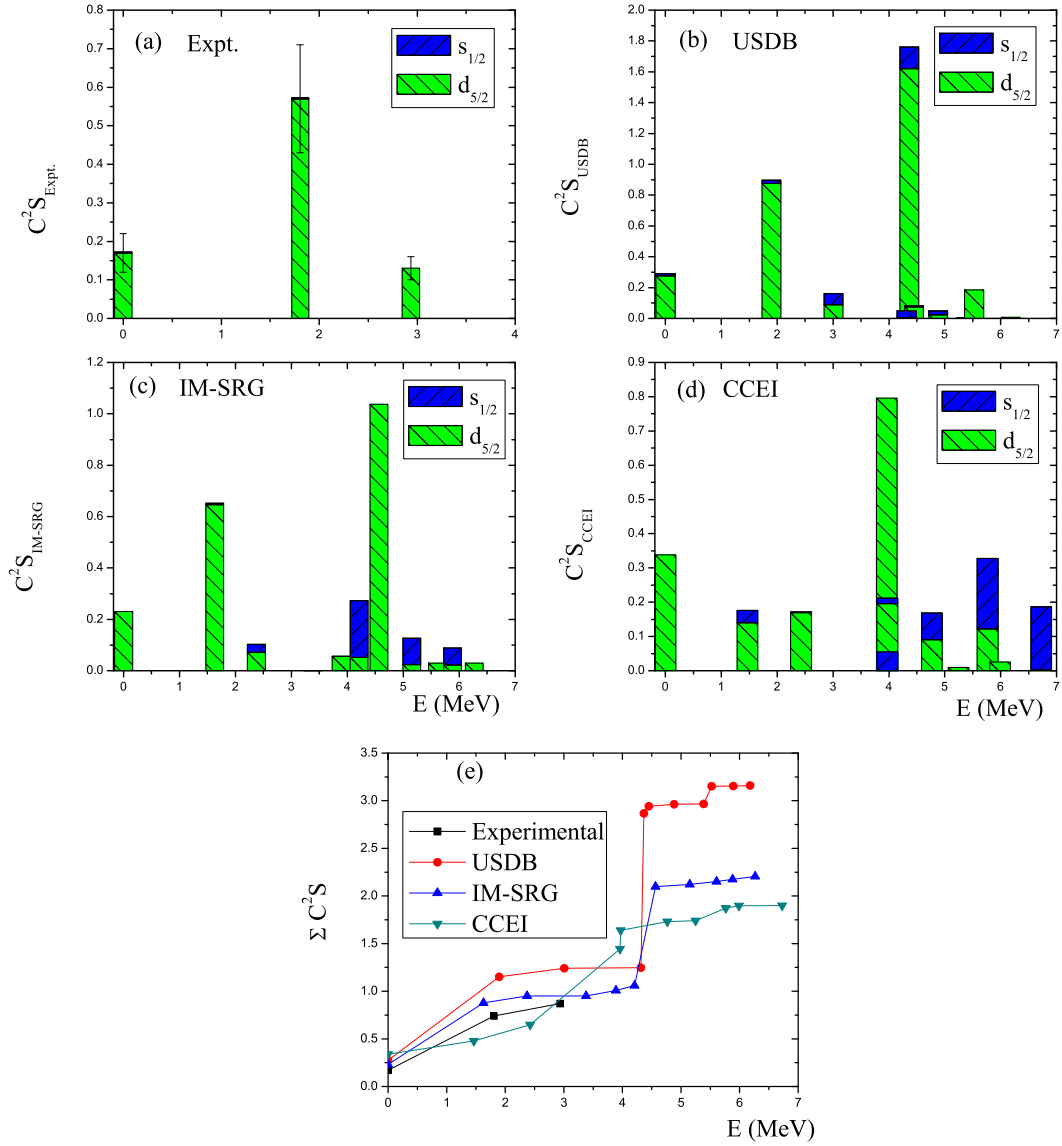

FIG. 3. C^2S comparison between calculated and extracted values from experimental data using the zero-range DWBA model calculation [17] for ^{26}Mg.

TABLE II. Wave functions of different states for ^{26}Mg. The SFs corresponding to these states are shown in Table I.

J^π	IM-SRG		USDB	
	%	Configuration	%	Configuration
0^+	49	$\pi(d_{5/2})^4\otimes\nu(d_{5/2})^6$	62	$\pi(d_{5/2})^4\otimes\nu(d_{5/2})^6$
2^+	43	$\pi(d_{5/2})^4\otimes\nu(d_{5/2})^6$	52	$\pi(d_{5/2})^4\otimes\nu(d_{5/2})^6$
2^+	29	$\pi(d_{5/2})^3(s_{1/2})^1\otimes\nu(d_{5/2})^5(s_{1/2})^1$	29	$\pi(d_{5/2})^4\otimes\nu(d_{5/2})^5(s_{1/2})^1$
3^+	33	$\pi(d_{5/2})^4\otimes\nu(d_{5/2})^5(s_{1/2})^1$	35	$\pi(d_{5/2})^4\otimes\nu(d_{5/2})^5(s_{1/2})^1$
4^+	35	$\pi(d_{5/2})^4\otimes\nu(d_{5/2})^6$	52	$\pi(d_{5/2})^4\otimes\nu(d_{5/2})^6$
2^+	23	$\pi(d_{5/2})^4\otimes\nu(d_{3/2})^1(d_{5/2})^4(s_{1/2})^1$	25	$\pi(d_{5/2})^4\otimes\nu(d_{5/2})^6$
2^+	28	$\pi(d_{5/2})^3(s_{1/2})^1\otimes\nu(d_{5/2})^6$	33	$\pi(d_{5/2})^3(s_{1/2})^1\otimes\nu(d_{5/2})^6$
2^+	22	$\pi(d_{5/2})^4\otimes\nu(d_{3/2})^1(d_{5/2})^5$	33	$\pi(d_{5/2})^4\otimes\nu(d_{3/2})^1(d_{5/2})^5$
4^+	31	$\pi(d_{5/2})^4\otimes\nu(d_{5/2})^5(s_{1/2})^1$	26	$\pi(d_{5/2})^4\otimes\nu(d_{5/2})^5(s_{1/2})^1$
4^+	29	$\pi(d_{5/2})^4\otimes\nu(d_{5/2})^4(s_{1/2})^2$	31	$\pi(d_{5/2})^4\otimes\nu(d_{5/2})^5(s_{1/2})^1$
3^+	32	$\pi(d_{5/2})^4\otimes\nu(d_{3/2})^1(d_{5/2})^5$	50	$\pi(d_{5/2})^4\otimes\nu(d_{5/2})^5(s_{1/2})^1$

TABLE III. Extracted values of C^2S for different excited states of ^{26}Al from the reaction ^{27}Al(d,t). Experimental data are from Ref. [25]. Here $l=0$ and $l=2$ are for $s_{1/2}$ and $d_{5/2}$ orbitals, respectively.

Expt.	J^π	[USDB]	[IM-SRG]	[CCEI]	C^2S[Expt.]		C^2S[USDB]		C^2S[IM-SRG]		C^2S[CCEI]	
keV		keV	keV	keV	$l=0$	$l=2$	$l=0$	$l=2$	$l=0$	$l=2$	$l=0$	$l=2$
0	5^+_1	$0(5^+_1)$	$247(5^+_1)$	$838(5^+_1)$		0.73 ± 0.21		1.089		0.811		0.627
228.3	0^+_1	$229(0^+_1)$	$903(0^+_1)$	$2563(0^+_2)$		0.09 ± 0.03		0.139		0.117		0.004
416.8	3^+_1	$520(3^+_1)$	$1963(3^+_2)$	$1873(3^+_3)$		0.32 ± 0.07	0.201	0.0001	0.0003	0.321	0.028	0.004
1057.7	1^+_1	$1034(1^+_1)$	$1853(1^+_3)$	$1224(1^+_3)$		0.17 ± 0.05		0.004		0.0007		0.114
1759.0	2^+_1	$1583(2^+_1)$	$1691(2^+_2)$	$1704(2^+_3)$		0.038 ± 0.006	0.031	0.004	0.001	0.0001	0.046	0.023
1850.6	1^+_2	$1818(1^+_2)$	$2399(1^+_4)$	$3497(1^+_5)$		0.019 ± 0.004	0.007	0.438		0.001		0.027
2068.8	2^+_2	$2126(2^+_2)$	$2530(2^+_3)$	$2757(2^+_4)$		0.26 ± 0.06	0.007	0.438	0.0004	0.002	0.007	0.146
2365.1	3^+_2	$2155(3^+_2)$	$2825(3^+_4)$	$2832(3^+_5)$		0.13 ± 0.02	0.008	0.310	0.0005	0.005	0.022	0.071
2545.3	3^+_3	$2402(3^+_3)$	$3466(3^+_5)$	$3260(3^+_6)$		0.16 ± 0.03	0.002	0.120	0.001	0.008	0.049	0.068
3159.8	2^+_3	$3236(2^+_5)$	$3404(2^+_6)$	$3853(2^+_6)$		0.06 ± 0.01	0.010	0.045	0.016	0.051	0.000	0.068
3402.6	5^+_2	$3398(5^+_2)$	$3496(5^+_2)$	$4223(5^+_3)$		0.06 ± 0.01		0.077		0.133		0.0007
4705.3	4^+_1	$4857(4^+_5)$	$5282(4^+_5)$	$4704(4^+_5)$		0.27 ± 0.08		0.0003		0.007		0.008

TABLE IV. Wave functions of different states for ^{26}Al. The SFs corresponding to these states are shown in Table III.

J^π	IM-SRG		USDB	
	%	Configuration	%	Configuration
5^+	48	$\pi(d_{5/2})^5\otimes\nu(d_{5/2})^5$	62	$\pi(d_{5/2})^5\otimes\nu(d_{5/2})^5$
0^+	54	$\pi(d_{5/2})^5\otimes\nu(d_{5/2})^5$	65	$\pi(d_{5/2})^5\otimes\nu(d_{5/2})^5$
3^+	23	$\pi(d_{5/2})^4(s_{1/2})^1\otimes\nu(d_{5/2})^4(s_{1/2})^1$	18	$\pi(d_{5/2})^4(s_{1/2})^1\otimes\nu(d_{5/2})^5$
1^+	15	$\pi(d_{5/2})^4(s_{1/2})^1\otimes\nu(d_{5/2})^4(s_{1/2})^1$	57	$\pi(d_{5/2})^5\otimes\nu(d_{5/2})^5$
2^+	13	$\pi(d_{3/2})^1(d_{5/2})^4\otimes\nu(d_{5/2})^4(s_{1/2})^1$	16	$\pi(d_{3/2})^1(d_{5/2})^4\otimes\nu(d_{5/2})^5$
1^+	16	$\pi(d_{5/2})^4(s_{1/2})^1\otimes\nu(d_{5/2})^4(s_{1/2})^1$	19	$\pi(d_{5/2})^4(s_{1/2})^1\otimes\nu(d_{5/2})^4(s_{1/2})^1$
2^+	14	$\pi(d_{3/2})^1(d_{5/2})^4\otimes\nu(d_{5/2})^5$	42	$\pi(d_{5/2})^5\otimes\nu(d_{5/2})^5$
3^+	17	$\pi(d_{3/2})^1(d_{5/2})^4\otimes\nu(d_{3/2})^1(d_{5/2})^4$	30	$\pi(d_{5/2})^5\otimes\nu(d_{5/2})^5$
3^+	14	$\pi(d_{3/2})^1(d_{5/2})^4\otimes\nu(d_{5/2})^5$	21	$\pi(d_{5/2})^5\otimes\nu(d_{5/2})^5$
2^+	18	$\pi(d_{5/2})^5\otimes\nu(d_{5/2})^4(s_{1/2})^1$	13	$\pi(d_{5/2})^4(s_{1/2})^1\otimes\nu(d_{5/2})^4(s_{1/2})^1$
5^+	16	$\pi(d_{5/2})^5\otimes\nu(d_{5/2})^5$	17	$\pi(d_{5/2})^5\otimes\nu(d_{5/2})^5$
4^+	24	$\pi(d_{5/2})^5\otimes\nu(d_{5/2})^4(s_{1/2})^1$	17	$\pi(d_{5/2})^5\otimes\nu(d_{5/2})^4(s_{1/2})^1$

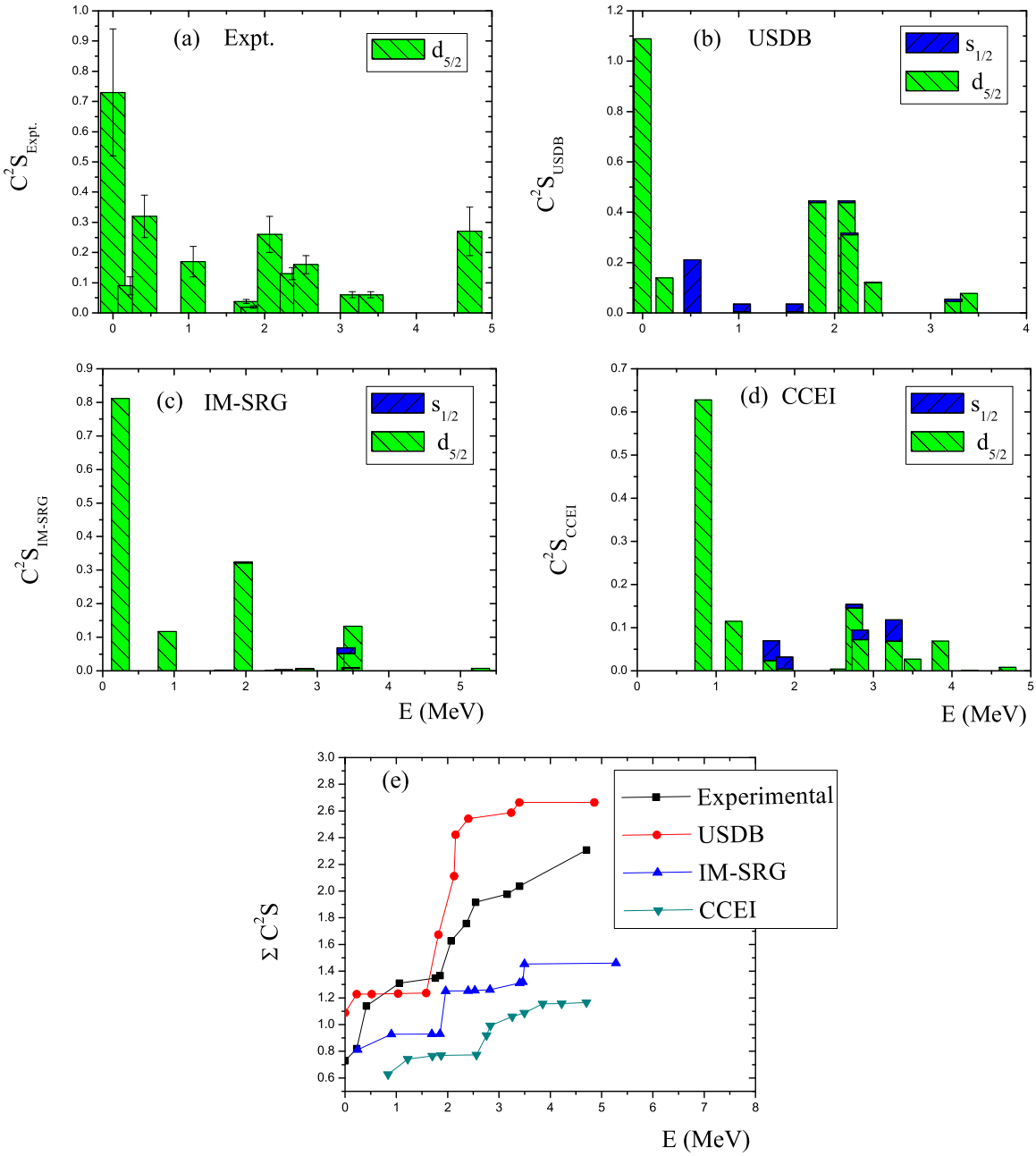

FIG. 4. C^2S comparison between calculated and extracted values from experimental data using the zero-range DWBA model calculations [25] for ^{26}Al.

($s_{1/2}$) transfer. The shell-model results are larger for the first two states, thus assigning larger single-particle characteristics to these states. In the present work we have also predicted C^2S values for states up to ∼6 MeV. In Figs. 3(a)–3(d) we show the variation of C^2S for extracted experiment and calculated values. In all three shell-model calculations, the spectroscopic factor for pickup from the $s_{1/2}$ orbital plays a major role for the higher excited states. In Fig. 3(e), we also plotted $\sum C^2S$ values for theory and extracted experimental values. The $\sum C^2S$ values calculated from IM-SRG and CCEI interactions show the same trends as the extracted values from the experiment.

B. Calculation of C^2S for 1*n* pick-up reaction ^{27}Al$(d,t)^{26}$Al

The states of ^{26}Al [25] were experimentally studied by assuming pick-up from $d_{5/2}$ and $s_{1/2}$ single-particle orbitals, while the 6^+ state at 3507 keV by assuming pick-up from the $g_{9/2}$ orbital. In Table III, we compared experimental C^2S values with shell-model results for IM-SRG, CCEI, and USDB interactions. The experimentally extracted values for spectroscopic factors up to ∼4.7 MeV are reported in Ref. [25]. In the present work we interpreted these extracted SFs in terms of the shell-model calculations (the corresponding wave functions are shown in Table IV). The experimental C^2S values for $d_{5/2}$ states are given in Table III. For the 5^+ state the SF

results with IM-SRG and USDB are slightly higher than the extracted experimental value, while it is smaller with CCEI. For some states the SFs are very small because in those cases the wave functions are very fragmented. This is because of large cancellations of contributions from different components of the wave functions. For 2^+ at 1759 keV and 4^+ at 4705 keV, the IM-SRG, CCEI, and USDB interactions predict very small values for the spectroscopic factors.

In Figs. 4(a)–4(d) we show the variation of C^2S for extracted experimental and calculated values. In Fig. 4(e), we also plot the $\sum C^2S$ values for theory and extracted experimental values. The extracted experimental $\sum C^2S$ values show a good trend with IM-SRG and CCEI results.

III. SUMMARY

We performed shell-model calculations for spectroscopic factors with two *ab initio* approaches: an in-medium similarity renormalization targeted for a particular nucleus and coupled-cluster effective interaction (CCEI). We also performed calculations with the realistic USDB effective interaction. Along with the *ab initio* results, we present a comparison with recently determined experimental spectroscopic factors.

ACKNOWLEDGMENTS

P.C.S. thanks P. Navrátil and S. R. Stroberg for useful discussions during this work. We also thank R. Shyam and V. K. B. Kota for useful comments to improve this manuscript. P.C.S. acknowledges the hospitality extended to him during his stay at TRIUMF, Vancouver City, Canada. P.C.S. acknowledges financial support from faculty initiation grants. V.K.'s work was supported in part by the CSIR Grant No. 09/143(0844)/2013-EMR-1 - India Ph.D. fellowship program.

[1] P. J. Brussaard and P. W. M. Glaudemans, *Shell-Model Applications in Nuclear Spectroscopy* (North-Holland, Amsterdam, 1977).
[2] M. H. Macfarlane and J. B. French, Rev. Mod. Phys. **32**, 567 (1960).
[3] J. P. Schiffer, S. J. Freeman, J. A. Clark, C. Deibel, C. R. Fitzpatrick, S. Gros, A. Heinz, D. Hirata, C. L. Jiang, B. P. Kay, A. Parikh, P. D. Parker, K. E. Rehm, A. C. C. Villari, V. Werner, and C. Wrede, Phys. Rev. Lett. **100**, 112501 (2008).
[4] J. P. Schiffer, C. R. Hoffman, B. P. Kay, J. A. Clark, C. M. Deibel, S. J. Freeman, A. M. Howard, A. J. Mitchell, P. D. Parker, D. K. Sharp, and J. S. Thomas, Phys. Rev. Lett. **108**, 022501 (2012).
[5] B. A. Brown, P. G. Hansen, B. M. Sherrill, and J. A. Tostevin, Phys. Rev. C **65**, 061601(R) (2002).
[6] M. B. Tsang, J. Lee, and W. G. Lynch, Phys. Rev. Lett. **95**, 222501 (2005).
[7] P. Morfouace *et al.*, Phys. Lett. B **751**, 306 (2015).
[8] J. Lee, M. B. Tsang, and W. G. Lynch, Phys. Rev. C **75**, 064320 (2007).
[9] M. B. Tsang, J. Lee, S. C. Su, J. Y. Dai, M. Horoi, H. Liu, W. G. Lynch, and S. Warren, Phys. Rev. Lett. **102**, 062501 (2009).
[10] J. Vernotte, G. Berrier-Ronsin, S. Fortier, E. Hourani, J. Kalifa, J. M. Maison, L. H. Rosier, G. Rotbard, and B. H. Wildenthal, Phys. Rev. C **48**, 205 (1993).
[11] B. H. Wildenthal *et al.*, Phys. Rev. **175**, 1431 (1968).
[12] G. J. Wagner *et al.*, Nucl. Phys. A **125**, 80 (1969).
[13] M. Arditi *et al.*, Nucl. Phys. A **165**, 129 (1969).
[14] J. J. Kraushaar, M. Fujiwara, K. Hosono, H. Ito, M. Kondo, H. Sakai, M. Tosaki, M. Yasue, S. I. Hayakawa, and R. J. Peterson, Phys. Rev. C **34**, 1530 (1986).
[15] M. Yasue, K. Ogawa, T. Niizeki, J. Takamatsu, M. Ohura, A. Terakawa, T. Nakagawa, T. Hasegawa, H. Ohnuma, H. Toyokawa, and S. Hamada, Phys. Rev. C **42**, 1279 (1990).
[16] M. Burlein, K. S. Dhuga, and H. T. Fortune, Phys. Rev. C **29**, 2013 (1984).
[17] V. Srivastava, C. Bhattacharya, T. K. Rana, S. Manna, S. Kundu, S. Bhattacharya, K. Banerjee, P. Roy, R. Pandey, G. Mukherjee, T. K. Ghosh, J. K. Meena, T. Roy, A. Chaudhuri, M. Sinha, A. K. Saha, M. A. Asgar, A. Dey, S. Roy, and M. M. Shaikh, Phys. Rev. C **93**, 044601 (2016).
[18] K. A. Chipps, D. W. Bardayan, K. Y. Chae, J. A. Cizewski, R. L. Kozub, C. Matei, B. H. Moazen, C. D. Nesaraja, P. D. O'Malley, S. D. Pain, W. A. Peters, S. T. Pittman, K. T. Schmitt, and M. S. Smith, Phys. Rev. C **86**, 014329 (2012).
[19] N. Takahashi, Y. Hashimoto, Y. Iwasaki, K. Sakurai, F. Soga, K. Sagara, Y. Yano, and M. Sekiguchi, Phys. Rev. C **23**, 1305 (1981).
[20] J. Kroon *et al.*, Nucl. Phys. A **204**, 609 (1973).
[21] D. L. Show *et al.*, Nucl. Phys. A **263**, 293 (1977).
[22] R. R. Betts *et al.*, Phys. Rev. C **8**, 670 (1972).
[23] J. Nurzynski *et al.*, Nucl. Phys. A **107**, 581 (1968).
[24] N. A. Vlasov, S. P. Kalinin, A. A. Ogloblin, and V. I. Chuev, JETP (Sov. Phys.) **10**, 844 (1960).
[25] V. Srivastava, C. Bhattacharya, T. K. Rana, S. Manna, S. Kundu, S. Bhattacharya, K. Banerjee, P. Roy, R. Pandey, G. Mukherjee, T. K. Ghosh, J. K. Meena, T. Roy, A. Chaudhuri, M. Sinha, A. Saha, M. A. Asgar, A. Dey, S. Roy, and M. M. Shaikh, Phys. Rev. C **91**, 054611 (2015).
[26] R. Diehl *et al.*, Nature (London) **439**, 45 (2006).
[27] S. R. Stroberg *et al.*, arXiv:1607.03229v1; private communication.
[28] G. R. Jansen, M. D. Schuster, A. Signoracci, G. Hagen, and P. Navrátil, Phys. Rev. C **94**, 011301(R) (2016); G. R. Jansen, J. Engel, G. Hagen, P. Navrátil, and A. Signoracci, Phys. Rev. Lett. **113**, 142502 (2014).
[29] B. A. Brown and W. A. Richter, Phys. Rev. C **74**, 034315 (2006).
[30] B. A. Brown, W. D. M. Rae, E. McDonald, and M. Horoi, NushellX@MSU.
[31] S. R. Stroberg, H. Hergert, J. D. Holt, S. K. Bogner, and A. Schwenk, Phys. Rev. C **93**, 051301(R) (2016).
[32] O. Jensen, G. Hagen, T. Papenbrock, D. J. Dean, and J. S. Vaagen, Phys. Rev. C **82**, 014310 (2010).
[33] W. A. Richter and B. A. Brown, Phys. Rev. C **80**, 034301 (2009).
[34] A. Poves, http://www.cenbg.in2p3.fr/heberge/EcoleJoliotCurie/coursannee/cours/CoursPoves.pdf.
[35] B. A. Brown, Lecture Notes in Nuclear Structure Physics, www.nscl.msu.edu/~brown/Jina-workshop/BAB-lecture-notes.pdf.
[36] A. A. Ioannides, M. A. Nagarajan, and R. Shyam, Nucl. Phys. A **363**, 150 (1981).

[37] A. A. Ioannides, M. A. Nagarajan, and R. Shyam, Phys. Lett. B **103**, 187 (1981).
[38] M. A. Nagarajan and R. Shyam, Phys. Rev. C **26**, 977 (1982).
[39] R. J. Furnstahl and H.-W. Hammer, Phys. Lett. B **531**, 203 (2002).
[40] R. J. Furnstahl and A. Schwenk, J. Phys. G: Nucl. Part. Phys. **37**, 064005 (2010).
[41] C. Barbieri, Phys. Rev. Lett. **103**, 202502 (2009).
[42] W. H. Dickhoff and C. Barbieri, Prog. Part. Nucl. Phys. **52**, 377 (2004).